Design of Stable Nanoporous Hybrid Chitosan/Titania as Cooperative Bifunctional Catalysts

Abdelkrim El Kadib,[†] Karine Molvinger,*[,†] Claude Guimon,[‡] Françoise Quignard,[†] and Daniel Brunel[†]

Matériaux Avancés pour la Catalyse et la Santé, "MACS", Institut Charles Gerhardt, UMR 5253 CNRS/ENSCM/UM2/UM1, 8 rue de l'Ecole Normale, 34296 Montpellier Cedex 5, France, and IPREM/ECP−UMR CNRS 5254, Helioparc Pau-Pyrenees, 2 Avenue P. Angot, 64053 Pau Cedex 9, France

Received September 25, 2007. Accepted January 17, 2008

A new method describing the synthesis of hybrid porous materials based on chitosan/titania featuring high surface area and shaped as microspheres is reported. The particular self-assembly properties of chitosan in addition to the mutual chemical interaction between the glucosamine units and the titania precursors control the titania condensation inside the beads of chitosan. The intimate mixing of organic and inorganic frameworks entails a notable improvement on the hydrolytic stability of resulting material when compared to the individual component ones. Moreover, highly active and selective catalytic properties for monoglyceride synthesis stems from the coexistence of the basic sites (NH_2 from biopolymer) and acid sites (titanium center) through their cooperative effect.

Introduction

Inspired by the efficiency, elegance, and selectivity of enzymatic catalysis, the design of catalysts capable of the efficient promotion of synthetic processes is a challenge which is currently receiving considerable attention.[1] In this context, one of the fundamental enzymatic catalyst assets, which is the most difficult to engineer in synthetic systems, is the cooperative bifunctionality, which means the ability of a catalyst to synergistically supply to the nucleophilic and electrophilic components with a simultaneous activation by its Lewis/Brönsted acidic and Lewis/Brönsted basic functionality.[2] Surprisingly, despite the abundant literature addressing this topics, there are few reports on bifunctional[3] heterogeneous hybrid catalysis based on the concomitant presence of acid and base sites on the same solid.[4,5] Solid catalysts provide numerous opportunities for recovering and recycling catalysts from reaction environments.[6] These features are crucial to improve processing steps, better economical processes, and environmentally friendly industrial manufacturing. Indeed, the development of biopolymer/inorganic oxide materials has become of great interest since 15 years.[7] In the literature, different polysaccharides/mineral oxides are described such as cellulose/silica,[8] alginate/silica,[9] chitosan/silica,[10] and cellulose/titania.[11] We mostly focused our works on chitosan consisting in a copolymer of linked

* Corresponding author. E-mail: karine.molvinger@enscm.fr. Fax: 33 (0)467163470.
[†] UMR 5253 CNRS/ENSCM/UM2/UM1.
[‡] IPREM/ECP−UMR CNRS 5254.

(1) (a) Dalko, P. I.; Moisan, L. *Angew. Chem.* **2004**, *116*, 5248–5286. (b) Houk, K. N.; List, B. *Acc. Chem. Res.* **2004**, *37*, 287–287. (c) Seayad, J.; List, B. *Org. Biomol.Chem.* **2005**, *3*, 719–724.

(2) (a) Okino, T.; Hoashi, Y.; Furukawa, T.; Xu, X.; Takemoto, Y. *J. Am. Chem. Soc.* **2005**, *127*, 119–125. (b) Hoashi, Y.; Okino, T.; Takemoto, Y. *Angew. Chem.* **2005**, *117*, 4100–4103. Angew. Chem. Int. Ed. 2005, 44, 4032–4035. (c) Dove, A. P.; Pratt, R. C.; Lohmeijer, B. G. G.; Waymouth, R. M.; Hedrick, J. L. *J. Am. Chem. Soc.* **2005**, *127*, 13798–13799. (d) Berkessel, A.; Cleemann, F.; Mukherjee, S.; Muller, T. N.; Lex, J. *Angew. Chem.* **2005**, *117*, 817–821. Angew. Chem. Int. Ed. 2005, 44, 807–811. (e) Song, J.; Wang, Y. *J. Am. Chem. Soc.* **2006**, *128*, 6048–6049. (f) Liu, T. Y.; Li, R.; Chai, Q.; Long, J.; Li, B. J.; Wu, Y.; Ding, L. S.; Chen, Y. C. *Chem.−Eur. J.* **2007**, *13*, 319–327.

(3) (a) Sinfelt, J. H.; Drew, T. B.; Hoopes Jr, J. W.; Vermeulen, T. *Adv. Chem. Eng.* **1964**, *5*, 37–74, and refs therein. (b) Gallezot, P. *Catal. Rev.−Sci. Eng.* **1979**, *20*, 121–153. (c) Panagiotis, P. G.; Ruckenstein, E. *J. Catal.* **1993**, *140*, 526–542. (d) GjervanT. PrestvikR. HolmenA. *Springer Series in Chemical Physics*; Springer-Verlag Publisher: Berlin, 2004; Vol. 75, pp 127−158, and refs therein. (e) Sun, Q.; Auroux, A.; Shen, J. *J. Catal.* **2006**, *244*, 1–9.

(4) (a) Tsuji, H.; Yagi, F.; Hattori, H.; Kita, H. *J. Catal.* **1994**, *148*, 759–770. (b) Climent, M. J.; Corma, A.; Garcia, H.; Guil-Lopez, R.; Iborra, S.; Fornés, V. *J. Catal.* **2001**, *197*, 385–393. (c) Climent, M. J.; Corma, A.; Iborra, S.; Velty, A. *J. Mol. Catal. A: Chem.* **2002**, *182–183*, 327–342. (d) Climent, M. J.; Corma, A.; Fornes, V.; Guil-Lopez, R.; Iborra, S. *Adv. Synth. Catal.* **2002**, *344*, 1090–1096. (e) Bass, J. D.; Anderson, S. L.; Katz, A. *Angew. Chem.* **2003**, *115*, 5377–5380. Angew. Chem. Int. Ed. 2003, 42, 5219–5222. (f) Figueras, F. *Top. Catal.* **2004**, *29*, 189–196. (g) Notestein, J. M.; Katz, A. *Chem.−Eur. J.* **2006**, *12*, 3954–3965.

(5) Gelman, F.; Blum, J.; Avnir, D. *Angew. Chem.* **2001**, *113*, 3759−3761; *Angew. Chem., Int. Ed.* **2001**, *40*, 3647−3649.

(6) (a) Clark, J. H.; Rhodes, C. N. *Clean Synthesis Using Porous Inorganic Solid Catalysts and Supported Reageants*; Royal Society of Chemistry: Cambridge, U.K., 2000. (b) De Vos, D. E.; Vankelecom, I. F. J.; Jacobs, P. A. *Chiral Catalyst Immobilization and Recycling*; Wiley-VCH: New York, 2000. (c) Sheldon, R. A.; van Bekkum, H. *Fine Chemicals through Heterogeneous Catalysis*; Wiley-VCH: Weinhem, Germany, 2001. (d) Gladysz, J. A. *Chem. Rev.* **2002**, *102*, 3215–3216.

(7) (a) Sanchez, C.; Lebeau, B.; Ribot, F.; In, M. *J. Sol−Gel Sci. Technol.* **2000**, *19*, 31–38. (b) Shchipunov, Y. A.; Karpenko, T. Y.; Krekoten, A. *Compos. Interfaces* **2005**, *11*, 587–607.

(8) Sequeira, S.; Evtuguin, D. V.; Portugal, I.; Esculcas, A. P. *Mater. Sci. Eng.* **2007**, *27*, 172–179.

(9) Coradin, T.; Livage, J. *J. Sol−Gel Sci. Technol.* **2003**, *26*, 1165–1168.

(10) (a) Muzzarelli, C.; Muzzarelli, R. A. A. *J. Inorg. Biochem.* **2002**, *92*, 89–94. (b) Yeh, J.-T.; Chen, C.-L.; Huang, K.-S. *Mater. Lett.* **2007**, *61* (6), 1292–1295. (c) Ayers, M. R.; Hunt, A. J. *J. Non-Cryst. Solids* **2001**, *285* (1–3), 123–127. (d) Silva, S. S.; Ferreira, R. A. S.; Fu, L.; Carlos, L. D.; Mano, J. F.; Reis, R. L.; Rocha, J. *J. Mater. Chem.* **2005**, *15* (35–36), 3952–3961.

(11) (a) Nagaoka, S.; Arinaga, K.; Kubo, H.; Hamaoka, S.; Sakurai, T.; Takafuji, M.; Ihara, H. *Polym. J.* **2005**, *37*, 186–191. (b) Marques, P.A.A.P.; Trindade, T.; Neto, C. P. *Compos. Sci. Technol.* **2006**, *66*, 1038–1044.

10.1021/cm800080s CCC: $40.75 © 2008 American Chemical Society
Published on Web 02/27/2008

Scheme 1. Chemical Structure of Chitosan

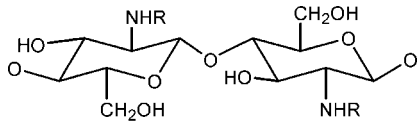

R: H, $COCH_3$

β,(1→4),2-amino-2-deoxy-D-glucan and 2-acetamidodeoxy-D-glucan resulting from uncomplete deacetylation of chitin (Scheme 1).

The biodegradability, natural abundance, and unlimited availability of chitin as a renewable agroressource make chitosan green material. Furthermore, chitosan is particularly attractive in regard to the presence of amino groups in most of their polymer units, for the preparation of hybrid and for its application in catalysis.[12] It is noteworthy that chitosan has been chemically modified to be performant as catalyst for achieving the most aimed process. For instance, amino groups were converted into Schiff bases and then into metal transition complexes that revealed excellent catalytic performance for hydrogenation or condensation reactions.[13] We have recently reported the direct use of chitosan beads as catalyst for the monoglyceride synthesis by fatty acid addition to glycidol.[12a] The performance of these materials was greatly improved by the texture tuning through supercritical CO_2 ($scCO_2$) drying. Afterward, porous chitosan-silica hybrid beads have been prepared by silica condensation inside $scCO_2$ dried chitosan microspheres in order to improve their textural and mechanical stabilities. Furthermore, this hybrid solid revealed also great potential as catalysts also for the monoglyceride synthesis.[12b] However, the major drawbacks that silica entails concern its hydrolytic instability, especially in basic conditions, and the absence of any functionality except the surface hydroxyl groups. The use of titania could circumvert these problems as titania reveals higher hydrolytic stability in basic conditions compare to silica.[14] Hence, titania turns out compatible with the proximity of chitosan amine groups and presents furthermore Lewis acidic sites. Besides their Lewis acidity, titania reveals also important interest for their specific properties in oxidation catalysis and photocatalysis.[15] In this work, we describe the synthesis of highly stable porous chitosan-titania hybrid featuring both basic site (NH_2) and Lewis acidic site (Ti) and its application as bifunctional catalysts for the monoglyceride synthesis. Thanks to the presence of these two different sites bore by each component in proximity, their cooperative interactions with both glycidol and fatty acid, which can easily access them, could induce a synergetic effect on the heterogeneous catalytic activity.

Experimental Section

Chitosan (Aldrich high molecular weight <25% acetylation) was used as the polymeric component. $Ti(acac)_2(iOPr)_2$ and $Ti(iOPr)_4$ (Aldrich) were used as precursor of titania.

Characterization of Materials. Nitrogen sorption isotherms at 77 K were obtained with a Micromeritics ASAP 2010 Micromeritics apparatus. Prior to measurement, the samples were degassed for 8 h at 80 °C. The surface area (S_{BET}) and the C_{BET} parameter were determined from BET treatment in the range 0.04–0.3 p/p_0[16] assuming a surface coverage of the nitrogen molecule estimated to 13.5 $Å^2$. The mesopore volume and the pore diameter were calculated using the nitrogen volume adsorbed when the capillary condensation is ended and the BdB model,[17] respectively. Thermogravimetric analyses were performed with a Netzsch TG 209 C apparatus. SEM images were obtained using a Hitachi S4500 microscope and EDX measurements were carried out using FEI 200F quanta 200F connected to the SEM Hitachi S4500 microscope. TEM images were obtained using JEOL 1200 EX II (120kV). DRIFT spectra were performed on Bruker vector 22. XPS analyses were performed at room temperature with an SSI 301 spectrometer using monochromatic and focused (spot diameter = 600 μm, 100 W) Al K α radiation (1486.6 eV) under a residual pressure of $\sim 1 \times 10^{-7}$ Pa. Charge effects were compensated by the use of a flood gun (5 eV). The hemispherical analyzer functioned at a constant pass energy of 50 eV. The experimental bands were fitted to theoretical bands (80% Gaussian, 20% Lorentzian) with a least-squares algorithm using a nonlinear baseline. Reference binding energy was C1s of CH_3 and of the contamination carbon at 284.6 eV. DRX were performed on D8 Advance Bruker AXS (powder diffraction, geometry: Bragg–Brentano). UV–visible (DRUV) spectra were measured in the 200–800 nm range using $BaSO_4$ as the reference on a Perkin-Elmer Lambda 14 spectrometer equipped with an integrating sphere (Labsphere, North Sutton, USA). Quartz cells (Hellma) of 0.05 mm path length were used. ^{13}C MAS NMR spectra were acquired on a Bruker Avance 300 DPX spectrometer operating at 75.467 MHz under cross-polarization conditions.

Synthesis of Chitosan Microspheres (M1**).** An aqueous solution of chitosan was obtained by dissolving 1g of chitosan in 100 mL of a solution of acetic acid (0.055 mol L^{-1}) corresponding to a stoechiometric amount of acid with respect to the amount of NH_2functions. Total dissolution was obtained under stirring over one night at room temperature. This solution was dropped into a NaOH solution (4N) through a 0.8 mm gauge syringe needle providing gelified chitosan microspheres. The chitosan beads were stored in the alkaline solution for 2 h and then dehydrated by immersion successively in a series of ethanol–water baths containing more and more ethanol until 100% ethanol bath. (these beads were directly used for the synthesis of **M3** and **M4**). The microspheres were then dried under supercritical CO_2 conditions (74 bar, 31.5 °C) in a Polaron 3100 apparatus (these beads were directly used for the synthesis of **M2**).

Synthesis of Chitosan/Titania Hybrid Microspheres. M2. The titania solution was prepared with $Ti(acac)_2(iOPr)_2$and isopropanol (Ti:iPrOH = 1:10). The beads of chitosan (M1) (250 mg) were suspended in the titania solution (4 mmol) at room temperature for 48 h. The microspheres were washed first with isopropanol twice

(12) (a) Valentin, R.; Molvinger, K.; Quignard, F.; Brunel, D. *New J. Chem.* **2003**, *27*, 1690–1692. (b) Molvinger, K.; Quignard, F.; Brunel, D.; Boissiere, M.; Devoisselle, J. M. *Chem. Mater.* **2004**, *16*, 3367–3372. (c) Guibal, E. *Prog. Polym. Sci.* **2005**, *30*, 71–109.
(13) (a) Hardy, J. J. E.; Hubert, S.; Macquarrie, D. J.; Wilson, A. J. *Green Chem.* **2004**, *6*, 53–56. (b) Macquarrie, D. J.; Hardy, J. J. E. *Ind. Eng. Chem. Res.* **2005**, *4423*, 8499–8520. (c) Yin, M.-Y.; Yuan, G.-L.; Wu, Y.-Q.; Huang, M. Y.; Jiang, Y. Y. *J. Mol. Catal. A: Chem.* **1999**, *147* (1–2), 93–98. (d) Corma, A.; Concepcion, P.; Dominguez, I.; Fornes, V.; Sabater, M. J. *J. Catal.* **2007**, *251*, 39–47.
(14) Brunel, D.; Mutin, P. H.; Blanc, A. C.; Lorret, O.; Lafond, V.; Galarneau, A.; Vioux, A.; Fajula, F. *Stud. Surf. Sci. Catal.* **2003**, *146*, 419–425.
(15) Hu, Y.; Ge, J.; Sun, Y.; Zhang, T.; Yin, Y. *Nano Lett.* **2007**, *7*, 1832–1836.
(16) Brunauer, S.; Emmet, P. H.; Teller, E. *J. Am. Chem. Soc.* **1938**, *60*, 309–319.
(17) Broekhoff, J. C. P.; De Boer, J. H. *J. Catal.* **1968**, *10*, 377–390.

Table 1. Textural Properties of Materials

catalyst	inorganic source	TiO_2 (%)[a]	Ti (%)[b]	BET area surface (m^2/g)	pore volume (cm^3/g)	pore diameter (Å)	*C*
M1		0	0	120	0.34	85	142
M2	$Ti(acac)_2(OiPr)_2$	3	0.7	30	0.25	206	47
M3	$Ti(acac)_2(OiPr)_2$	25	8.4	480	1.86	112	70
M4	$Ti(OiPr)_4$	29	11.4	450	1.29	71	58
M5[c]		100		308	0.87	108	94
M6[d]	TEOS			157	0.33	129	111

[a] Determined by TGA. [b] Atomic percent determined by EDX. [c] TiO_2 anatase form obtained from calcinated M3 at 450 °C for 8 h. [d] Percentage of SiO_2= 74% determined by TGA.

and then with ethanol. The hybrid microspheres were dried by supercritical CO_2.

M3 and M4. The titania solution was prepared with $Ti(acac)_2(iOPr)_2$ (M3) or $Ti(iOPr)_4$ (M4) and isopropanol (Ti:*i*PrOH = 1:10). The beads of chitosan swelled in ethanol (250 mg) were dipped in the titania solution (4 mmol) at room temperature for 48 h. The microspheres were washed first with isopropanol twice and then with ethanol. The hybrid microspheres were dried by supercritical CO_2.

Synthesis of Chitosan/Silica Hybrid Microspheres (M6**).** Hydrated chitosan microspheres (corresponding to 300 mg of dry chitosan) were put in an excess of tetraethoxysilane (0.12 mol of TEOS per gram of chitosan). The hydrolysis proceeded for 12 h. Fifty milligrams of NaF (1.2×10^{-3} mol) was added to catalyze the condensation of silica. The mixture maturated during 12 h. Then the beads were washed by distilled water and then dehydrated by immersion in a series of successive ethanol–water baths (150 mL). Additional absolute ethanol was used to accomplish complete exchange of the water in the microspheres by ethanol before drying under supercritical CO_2 ($scCO_2$) (73 bar, 31.5 °C) in a Polaron 3100 apparatus.

Catalytic Test. In a typical experiment: 0.5 mmol of lauric acid and 0.5 mmol of glycidol were injected in a flask containing 10% NH_2 catalyst (hybrid beads) in 4 mL of toluene. Zero time of reaction was taken when temperature reached 70 °C. Reagents and products amounts were determined by GC analysis (FID, HP5, T_{inj} = 250 °C, T_{det} = 275 °C, oven 50–250 °C, 15 °C min^{-1}) with octanol as internal standard according to a calibration curve established with authentic samples.

Results and Discussion

First, chitosan microspheres are prepared by inverse phase and dried by supercritical CO_2 according to the procedure already used previously (**M1,** Table 1).[12a] **M1** beads are impregnated by alcoholic $Ti(acac)_2(OiPr)_2$ solution (catalyst **M2**, Table 1). The loading of TiO_2 is only 3% and the surface area is low (S_{BET} = 30 m^2/g) compared to the parent sample (S_{BET} = 120 m^2/g). That could result from both shrinkage process during the polar solvent wetting and formation of titania mostly on the external bead surface which limits the diffusion of titanium species inside the chitosan microspheres. It has been reported that polysaccharide aerogel contains relatively high physisorbed water content (~17–20% mass loss at 373 K) upon contacting with air moisture during storage after the supercritical drying.[18] This would favor the plugging of the porosity entrance by fast titania formation through hydrolysis–condensation completing mostly at the external bead surface. To overcome this drawback, we use directly the alcogel microspheres, i.e., swollen polymeric chitosan resulting of the dialysis of the chitosan beads with 100% ethanol instead of $scCO_2$ dried chitosan microspheres (**M1**). Two titanium precursors ($Ti(acac)_2(OiPr)_2$ and $Ti(OiPr)_4$) (catalysts **M3** and **M4**, Table 1) are chosen in order to study the influence of hydrolysis and condensation rates on the physical and chemical properties of the materials, taking into account the lower reactivity of the former.[19] Whatever the titanium precursor nature, the surface area is very high (S_{BET} = 480 and 450 m^2/g), the higher surface that is reported up to now in the literature for polysaccharide based hybrid (see the Supporting Information, Figure S1). The more significant result is the strong enhancement of the surface area of the hybrids due to the addition of titanium oxide.

The loading of titania (25% for **M3** and 29% for **M4**), which is higher than the loading of titania in **M2**, demonstrated a better diffusion in the alcogel than in the aerogel as expected. Nitrogen adsorption/desorption isotherms of the hybrids (**M3** and **M4**) demonstrate similar feature that of the native chitosan one **M1**. These isotherms confirm the absence of microporosity, that might be created during the titania formation. All the hybrids are macroporous and have a monomodal pore size distribution. This result suggests that the Ti−O−Ti condensation inside the chitosan alcogel induces a sort of coating of chitosan fibers with the TiO_2, which decreases the texture shrinkage occurring during the change from alcogel to aerogel, although the $scCO_2$ drying lowers this phenomenom compare to the other methods of polysaccharide drying as for prestine chitosan.[20] By this method, the texture is remained after drying. Indeed, as previously shown, above the critical point, there is no interface, hence no meniscus tension; so the aerogel keeps the structure of the hydrogel, leading to a very high porosity by dispersion of the nanometric polysaccharide fibrils that form the aerogel scaffold. By contrast, the drying by evaporation brings to a dramatic shrinkage of the size and

(18) Horga, R.; Di Renzo, F.; Quignard, F. *Appl. Catal.* **2007**, *325*, 251–255.

(19) (a) Barringer, E. A.; Kent Bowen, H. *Langmuir* **1985**, *1*, 414–420. (b) Sanchez, C.; Livage, J.; Henry, M.; Babonneau, F. *J. Non-Cryst. Solids* **1988**, *100*, 65–76. (c) Léaustic, A.; Babonneau, F.; Livage, J. *Chem. Mater.* **1989**, *1*, 240–252, and 248–252.

(20) (a) Valentin, R.; Molvinger, K.; Quignard, F.; Di Renzo, F. *Macromol. Symp.* **2005**, *222*, 93–101. (b) Valentin, R.; Molvinger, K.; Viton, C.; Domard, A.; Quignard, F. *Biomacromolecules* **2005**, *6*, 2785–2792. (c) Boissiere, M.; Tourrette, A.; Devoisselle, J. M.; Di Renzo, F.; Quignard, F. *J. Colloid Interface Sci.* **2006**, *294* (1), 109–116. (d) Di Renzo, F.; Valentin, R.; Boissière, M.; Tourrette, A.; Sparapano, G.; Molvinger, K.; Devoisselle, J. M.; Gérardin, C.; Quignard, F. *Chem. Mater.* **2005**, *17*, 4693–4699. (e) Valentin, R.; Bonelli, B.; Garrone, E.; Di Renzo, F.; Quignard, F. *Biomacromolecules* **2007**, *8*, 3646–3650.

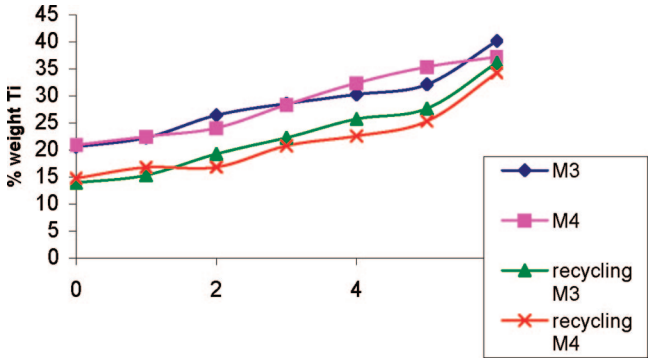

Figure 1. Radial distribution of hybrid materials.

surface properties, the porosity and morphology being crushed by capillary tension between polysaccharide structures.[20]

The values of the C parameter of these materials are given in the Table 1. C_{BET} parameter, were calculated using the Brunauer–Emmett–Teller model[16] in which $C_{BET} = \alpha \exp[(E_1 - E_L)/RT]$, where E_1 is the interaction energy between the surface and the first adsorbed layered of polarizable nitrogen molecule and E_L is the adsorption energy of nitrogen on the follower layers estimated to be the nitrogen liquefaction energy. Hence, C_{BET} coefficient has been associated to the surface polarity considering the interaction energy E_1 between the surface and the first adsorbed layered of polarizable nitrogen molecule,[21] but without taking into account the lateral intermolecular interaction. This assumption was furthermore confirmed by indirect contact angle measurement during water intrusion−extrusion studies with differently hydrophobized porous silica gels[22] and by surface polarity probing with Reichardt'dyes.[23] The very high C parameter value ($C = 142$) of chitosan alone **M1** is assigned to the presence of the numerous polar hydroxyl groups bore by the glucosamine units. For the hybrids, the hydrolysis/condensation of the titanium species consumes the hydroxyl groups of chitosan, thus leading to a decrease of the C parameter ($C = 70$ for **M3** and $C = 58$ for **M4**). The liberation of the chitosan by calcination leads to the formation of titania **M5** featuring surface Ti−OH groups that explain the subsequent increased value of the C parameter ($C = 94$).

The radial distribution of the titanium was determined by energy dispersive X-ray (EDX) microprobe analysis of a microsphere cross-section. These results indicate that, the titanium loading for both materials increases slightly toward the outer shell (Figure 1).

SEM and TEM analyses provide a clear representation of the structure of the composite materials **M3** and **M4** (Figures 2 and 3). The samples are spherical in shape and regular in size as shown on the photo picture (Figure 4). Observation of cross-sections shows a same network that in the native chitosan, a fibrous and macroporous structure. The homogeneity of the microspheres indicates that the materials does not present a core–shell structure. TEM analyses give a supplementary confirmation in nanoscale domain and show a homogeneous repartition of titanium particles (Figure 3). TEM photos show that the chitosan fibers seem to be petrified or fossilized by TiO_2 polymerization. The increase of the surface area of **M3** and **M4** can be explained by the fact that TiO_2 encircles the chitosan fibers in the form of a spiral, which leads to a roughness of the surface and by consequence an increase of the surface area. The fibrous aspect of titania could result from the coordination of the titanium alkoxyde by the amine groups of chitosan forming transient O*i*Pr-bridged dimers as already reported in the literature between titanium *tetra*isopropoxide and propylamine or 3-aminopropyltrialkoxysilane,[24] which can activate the titania precursors[19c] and favor a condensation direction leading to fibrous titania particles. The homogeneity of the materials and the shaping demonstrate hence, that chitosan behaves as directing agents to control mineral growth of titanium species. The hybrids are amorphous and there was no evidence of the presence of crystalline particles, in agreement with the absence of diffraction peaks in DRX analysis.

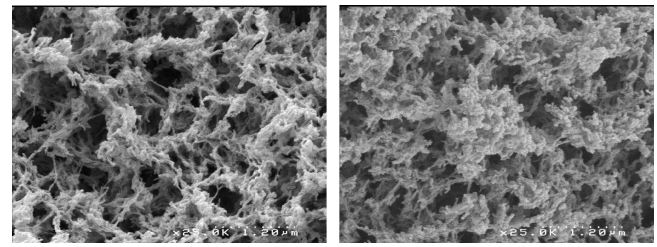

Figure 2. SEM of **M3** and **M4** hybrids.

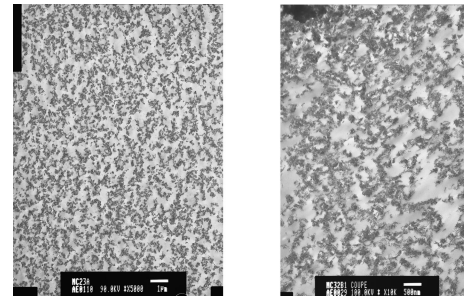

Figure 3. TEM of **M3** and **M4** hybrids.

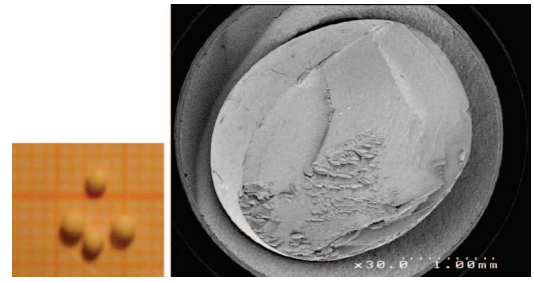

Figure 4. Photo of **M3** and SEM of transversal cut of **M4**.

(21) (a) Cauvel, A.; Brunel, D.; Di Renzo, F.; Fajula, F. *Am. Inst. Phys.* **1996**, *354*, 477–484. (b) Martin, T.; Galarneau, A.; Brunel, D.; Izard, V.; Hulea, V.; Blanc, A. C.; Abramson, S.; Di Renzo, F.; Fajula, F. *Stud. Surf. Sci. Catal.* **2001**, *135*, 4621–4628.

(22) (a) Martin, T.; Brunel, D.; Galarneau, A.; Di Renzo, F.; Fajula, F.; Lefevre, B.; Gobin, P. F.; Quinson, J. F.; Vigier, G. *Chem. Commun.* **2002**, 24–25. (b) Lefevre, B.; Gobin, P. F.; Martin, T.; Galarneau, A.; Brunel, D. *Mater. Res. Soc.* **2002**,April 1–5.

(23) Macquarrie, D. J.; Taverner, S. J.; Gray, G. W.; Heath, R. A.; Rafelt, J. S.; Saulzet, S. I.; Hardy, J. E.; Clark, J. H.; Sutra, P.; Brunel, D.; Di Renzo, F.; Fajula, F. *New J. Chem.* **1999**, *23*, 725–737.

(24) Fric, H.; Schubert, U. *New J. Chem.* **2005**, *29*, 232–236.

DRIFT analyses of titania/chitosan hybrid reveal the characteristic bands of chitosan (see the Supporting Information, Figure S2). The new bands observed at 1020 and 1158 cm^{-1} can be assigned to C−O−Ti.[25] The broadband below 800 cm^{-1} again confirms the presence of Ti−O−Ti.[26] In **M3**, the band at 1531 cm^{-1} is characteristic of acetylacetonato groups bound to titanium.[13]CP MAS NMR spectrum of **M3** and **M4** demonstrates characteristic signals of chitosan. In **M3**, two additional peaks at 118 and 195 ppm correspond to the acetylacetonate group of the titanium precursor. This NMR study is in agreement with the infrared results and shows clearly that alkoxy groups bridged to the titanium are hydrolyzed before acetylacetonato groups.[19b,c] DRUV analyses of **M3** and **M4** show a broad absorption band at 312 and 280 nm respectively, which are consistent with an incipient oligomerization of Ti(IV) species.[27] The XPS analyses of the different samples were performed in view to elucidate the nature species of titanium in these composite materials. First, XPS analyses revealing absorption peaks at 458.3 and 458.5 eV for **M3** and **M4**, respectively corroborated the presence of TiO_2 (see the Supporting Information, Figure S3).[28] Characteristic absorptions of CH_3 and CH_2 (284.6 eV) and of NH_2 (399 eV) are also shown (see the Supporting Information, Figures S4 and S5). Comparisons between the titanium concentration before and after grinding of the samples confirm the results obtained by EDX which indicates that the amount of titanium is more important in surface than inside the microspheres and that the titanium concentration is larger in **M4** than in **M3**. These analyses reveal two additional species: (i) a minoritary titanium species for **M3** only (457.3 eV), which is attributed to a titanium with a charge density slightly larger. One explanation consists in the difference between the condensation of titanium sources: $Ti(OiPr)_4$ and $Ti(acac)_2(OiPr)_2$. The condensation of $Ti(OiPr)_4$ is faster than the one of $Ti(acac)_2(OiPr)_2$. So the Ti(acac) complex remains in the material as observed by ^{13}C NMR. (ii) In **M4**, XPS reveals an additional peak at 401.1 eV attributed to the quaternized nitrogen NH_3^+ (18% compared to the amount of NH_2). Surprisingly, there is no significant signal at 396 eV (N1s) characteristics of coordination occurring between the nitrogen of chitosan and the titanium center, as expected taking into account the existence of coordination of the titanium alkoxyde by alkylamine groups.[24] This could be explains by a separation of the Lewis base-Lewis acid pair during the titania condensation, the O*i*Pr-bridged dimers existing only as transient species.

The stability of **M3** and **M4** samples was evaluated under acidic and basic conditions and compared with native chitosan **M1** and hybrid chitosan/silica beads **M6**. First, the samples were contacted with 0.1N of NaOH solution for 1 h. We observed crumbling of chitosan/silica **(M6)** under these conditions, explained by dissolution of silica part. This is supported by the decreasing of the inorganic part (16%) according to the TG analysis. This treatment also affects the texture of the hybrid (surface area of **M6** decreases dramatically from 157 to 84 m^2/g). The morphology of **M1** beads did not change even though their size slightly decreased. SEM analysis revealed condensed fibrous structure indicating that additional contraction occurs under basic conditions. In contrast, the morphology and size of chitosan/titania **M3** and **M4** were preserved. The composition of the hybrid remains the same as before the basic treatment. SEM analysis shows the fibrous structure of both materials. This evidences the higher hydrolytic stability of the hybrid chitosan/titania compared to the hybrid chitosan/silica, under basic conditions.[14] The stability under acidic conditions (0.1N of acetic acid) was also studied. Whereas chitosan/silica **M6** and native chitosan **M1** are completely dissolved, chitosan/titania beads remained unchanged. In the case of chitosan/silica hybrid, TG analysis reveals an increase of the inorganic part (10%), indicating the erosion of chitosan polymer by partial dissolution in acid media. As a consequence, the textural property of the chitosan/silica hybrid is also affected (surface area of **M6** decreases from 157 to 70 m^2/g). Interestingly, the composition of chitosan/titania remains the same even after 24 h in the acid solution. The fibrous morphology is preserved (see the SEM analysis in the Supporting Information, Figure S6). On the contrary, the inorganic titania and silica (obtained by calcinations of **M3** and **M6**, respectively) reveals poor stability both under acidic and basic conditions as shown by strong loss of texture ($S_{BET} < 5$ m^2/g) and particularly for silica by morphology modification (desintegration). So, chitosan/titania hybrid reveals higher hydrolytic stability compared to that of each individual component. This suggests intimate bond between organic and inorganic moieties. The hydrophilic properties of polysaccharides permit the uniform TiO_2 coating with high adhesivity.[29,30] Despite the protonation of amino groups leads to the dissolution of pure chitosan through breakage of the OH···N hydrogen bond, the titanium species located around the fibers of chitosan enhance the stability of these hybrid materials. The hydrogen bond was one of the combination strengths between chitosan and TiO_2[30] in addition to the existence of C−O−Ti bonds that maintained the cohesion of the hybrid schaffold. Moreover, the interfacial energy of each component solution could decrease by the mutual interaction between the two components, which brings a supplementary stabilizing effect to the hybrid system.[31]

We focused our attention to the study of catalytic activity of such materials. First, we studied the reaction of the fatty acid addition on glycidol (Scheme 2). The interest of this reaction is the formation of monoglyceride which are used

(25) Hu, Y.; Ge, J.; Sun, Y.; Zhang, T.; Yin, Y. *Nano Lett.* **2007**, *7*, 1832–1836.
(26) Jonggol, Jarupatrakorn.; Don Tilley, T. *J. Am. Chem. Soc.* **2002**, *124*, 8380–8388.
(27) (a) Marchese, L.; Gianotti, E.; Dellarocca, V.; Maschmeyer, T.; Rey, F.; Coluccia, S.; Thomas, J. M. *Phys. Chem. Chem. Phys.* **1999**, *1*, 585–592. (b) Hasegawa, Y.; Ayame, A. *Catal. Today* **2001**, *71*, 177–187. (c) Gianotti, E.; Frache, A.; Coluccia, S.; Thomas, J. M.; Maschmeyer, T.; Marchese, L. *J. Mol. Catal. A: Chem.* **2003**, *204–205*, 483–489.
(28) Wagner, C. D.; Riggs, W. M.; Davis, L. E.; Moulder, J. F.; Muilenberg, G. E. *Handbook of X-ray Photoelectron Spectroscopy*; Perkin-Elmer Corp.: Eden Prairie, MN, 1979; p 68.
(29) Goutailler, G.; Guillard, C.; Daniele, S.; Hubert-Pfalzgraf, L. G. *J. Mater. Chem.* **2003**, *13*, 342–346.
(30) Li, Q.; Su, H.; Tan, T. *Biochem. Eng. J.* **2007**, doi10.1016j.bej.2007.07.007.
(31) Jolivet, J. P.; Henry, M.; Livage, J. In *De la Solution à l'Oxyde*; Savoirs Actuels, InterEditions/CNRS: Paris, 1994; Chapter 8, pp 332–334..

Scheme 2. Monoglyceride Synthesis

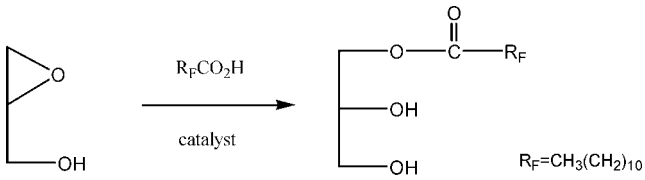

Table 2. Catalytic Formation of α-Monolaurin by Lauric Acid Addition on Glycidol

catalyst	reaction time (h)	Temperature (°C)	% conversion[a]	% selectivity[b]
M1	24	70	65	66
NH_2/SiO_2[24]	24	110	79[c]	89[c]
chitosan/SiO_2[12b]	50	70	82	65
M3 1st run	5	70	96	100
2nd run	7	70	90	100
3rd run	7	70	90	100
M4 1st run	5	70	76	100
2nd run	7	70	70	100
3rd run	7	70	70	100
M5	24	120	30	55

[a] Glycidol conversion. [b] Glycidol selectivity in α-monoglyceride formation. [c] Obtained after silanol passivation.

as emulsifiers in pharmacology and cosmetology domains. The reaction occurs via a nucleophilic ring opening of epoxy group leading to a monoacyl glycerol. The regioselective ring opening can be assisted by titanium isopropoxyde. The complexation of epoxy alcohol to the metal center, which acts as weak Lewis acid, enhances the rate and the regioselectivity of this reaction.[32] However, the necessity to use a large amount of titanium salts and the formation of byproducts is the major drawback of this process. Another method based on such reactions involves the use of amine functions as nucleophilic activating.[33] Under heterogeneous conditions, it has been previously shown that the primary or tertiary amines grafted onto silica successfully catalyzed this reaction in refluxing toluene as solvent.[34] In this work, the choice of chitosan is dictated by the presence of amino groups, which are potential base catalysts.[12] In addition, the use of titania in place of silica is a way to circumvent problems arising from the undesirable Bronsted acidity of silanol groups which leads to the polymerization of glycidol.[34]

Table 2 shows the results of the catalytic activity of the chitosan/titania hybrid microspheres. The reaction is carried out in toluene at 70 °C. We compared in this table the results obtained with previous catalysts.[12a,b,34] The samples **M3** and **M4** reveal a highly active and selective formation of monoglyceride. The first observation is that chitosan/titania samples prevent the glycidol polymerization. The energetic parameter of the BET equation (C_{BET}) for the two samples **M3** and **M4** is nearly lower than the native chitosan and calcined titanium as shown previously. On the basis of previous works, this suggests that the samples **M3** and **M4** are less polar than other catalysts.[21] This behavior is due to the consummation of hydrophilic groups (OH groups for

Scheme 3. Supposed Mechanism for Monoglycerid Synthesis

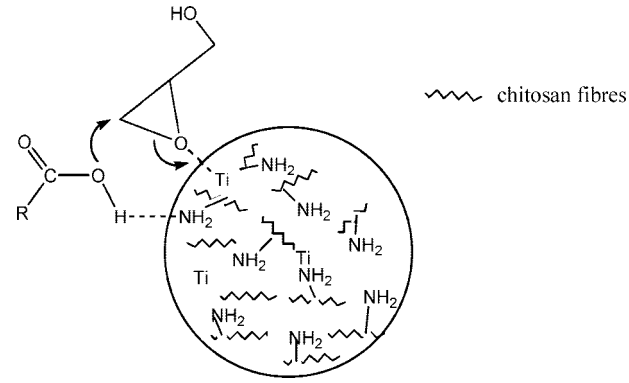

examples) during the diffusion and aggregation of titanium inside of beads. It has been reported that the presence of hydroxy groups is undesirable and leads to the polymerization of glycidol.[12b,34] In the case of amino catalysts based silica, the yield of monoglyceride is improved when the same catalysts are treated with hexamethyldisilazane, which is known to be reactive toward OH groups of various silicas.[34] It is noteworthy that the samples **M3** and **M4** showed also higher activity. After 5 h of reaction, high yield of monoglyceride was obtained (96 and 76%, respectively). First, the higher reactivity of **M3** compared to **M4** is due to the presence of Ti(acac) oligomers, which are expected to be more Lewis acid than the oligomers obtained from Ti(O*i*Pr)$_4$ condensation. Another explanation consists in the existence of NH_3^+ species in **M4** (18% with respect to NH_2 as observed by XPS analysis). The latter are less basic than NH_2, so the hydrogen abstraction of lauric acid is less efficient in the case of **M4** (compared to **M3**). Native chitosan (**M1**) is less active than chitosan/titania hybrids and gives moderate yield. Titania nanoparticles **M5** reveal a poor activity and selectivity toward monoglyceride formation. Other amorphous titania[35] are tested and the yield does not exceed 20%. The comparison of the results obtained from native chitosan **M1**, chitosan/titania (**M3** and **M4**) and titania nanoparticles **M5** demonstrates clearly the contribution of each site (basic or acid) in activation process. These results may be rationalized by the fact that the coexistence of nanotitania and amino groups in **M3** and **M4** might facilitate a synergic interaction between the functional groups and thereby lead to an efficient catalyst for monoglyceride synthesis. From mechanistic point of view, the following hypothesis may be reasonably formulated (Scheme 3): simultaneously, nucleophilic activating of lauric acid by abstraction of proton by basic site (NH_2 groups) and electrophilic activating of epoxy function by complexation with titanium metal centers facilitates a ring opening of epoxy group. This suggestion is consistent with the coexistence of separated Lewis base/Lewis acid sites inside the porous hybrid framework.

The recycling of the materials is tested. The results are given in Table 2. As can be seen there, a slightly loss of activity was observed. The analysis of the nitrogen adsorption isotherms shows a decreasing of specific BET surface area

(32) (a) Caron, M.; Sharpless, K. B. *J. Org. Chem.* **1985**, *50*, 1560–1563. (b) Burgos, C. E.; Ayer, D. E.; Johnson, R. A. *J. Org. Chem.* **1987**, *52*, 4973–4977.
(33) (a) Lok, C. M.; Ward, J. P.; van Dorp, D. A. *Chem. Phys. Lipids* **1976**, *16*, 115–122. (b) Lok, C. M.; Mank, A. P. J.; Ward, J. P. *Chem. Phys. Lipids* **1985**, *36*, 329–334.
(34) Cauvel, A.; Renard, G.; Brunel, D. *J. Org. Chem.* **1997**, *62*, 749–751.
(35) The blank samples were prepared by polymerization of Ti(acac)$_2$(O*i*Pr)$_2$ or Ti(O*i*Pr)$_4$ in isopropanol [1/10] leading to amorphous TiO_2.

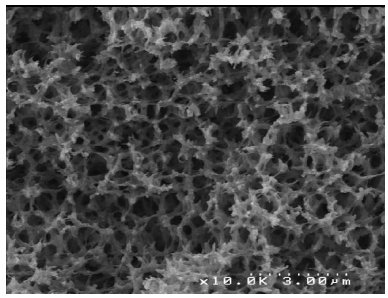

Figure 5. SEM of **M3** after 3 catalytic runs.

(S_{BET} = 142 m^2/g for **M3** and 110 m^2/g for **M4**), which may result from the filling of pores of catalysts by organic molecules or a shrinkage of the texture. Hence, total conversion of the reactants requires extended reaction time compared to the first run. Analysis of recycling materials by EDX shows a similar radial distribution than the parent samples (**M3** and **M4**) (Figure 1). XPS analyses show that the hybrid structure is not alterated even after three catalytic runs (see the Supporting Information). Finally, SEM photos show that the fibrous structures of samples are retained (Figure 5).

Conclusion

In summary, we reported the synthesis of highly porous chitosan/titania as bifunctional hybrid catalysts. The driving force of these catalysts is the accessibility of basic sites which are favored by $scCO_2$ drying and the homogeneous repartition of titania nanoparticles in the microspheres. During the preparation process, chitosan polymer behaves as a directing agent and control, by consequence, the growth of inorganic part. The presence of the latter around the fibers of organic polymer strongly enhances the stability of the resulting hybrid materials. The coexistence of amino groups as "nucleophilic activating" and titania nanoparticles as "electrophilic activating" leads to a highly active and selective heterogeneous catalysts for monoglyceride synthesis. The access to this hybrid materials based on titania opens opportunity for the future by extension of its application for soft and clean oxidation catalysis or photocatalysis for pollution remediation. Further works concerning the synthesis of other bifunctional hybrids (biopolymers/Lewis acids) and their catalytic activity are currently under investigation. In addition, the calcination of these hybrids constitutes an ingenious strategy to the elaboration of dispersed porous inorganic materials. This pathway is also in progess.

Acknowledgment. The authors are grateful to Rodolphe Guéret (UMR 5247, IBMM) for the NMR analysis and Didier Cot (IEM) and Thomas Cacciaguerra (ICGM-MACS) for the electronic microscopy. The authors thank also Carnot fundation for financial support.

Supporting Information Available: Figures S1−S6 (PDF). This material is available free of charge via the Internet at http://pubs.acs.org.

CM800080S